Respiration Physiology (1979) **36**, 1–17

GAS EXCHANGE ABNORMALITIES PRODUCED BY VENOUS GAS EMBOLI*

MICHAEL P. HLASTALA, H. THOMAS ROBERTSON and BRIAN K. ROSS

Departments of Medicine and of Physiology and Biophysics, University of Washington, Seattle, WA 98195, U.S.A.

Abstract. Bubbles of either He, N_2 or SF_6 were infused intravenously into anesthetized dogs at a rate of 0.2 ml/kg/min. Alterations in pulmonary gas exchange were quantitated by the inert gas elimination method during control, steady state infusion and resolution phases. The hypoxemia produced was predominantly due to regions of low $\dot{V}_A/\dot{Q}$ rather than pure shunt, and the increase in physiological dead space was due to the addition of high $\dot{V}_A/\dot{Q}$ regions rather than 'pure' dead space. The $\dot{V}_A/\dot{Q}$ distribution returned to normal within 30 minutes of stopping the He or N_2 bubbles, but remained abnormal for longer periods with SF_6 bubbles. The net elimination of insoluble gases (such as He or N_2) was only slightly impaired by bubble emboli, provided the cardiac output remained constant. Early pulmonary edema from bubble embolization was documented by increased wet weight/dry weight ratio, but the increased lung water was not apparent on histological examination. This form of pulmonary embolus is unique in that there is a constant fraction of the vasculature blocked although any given region with embolus is undergoing continuous resorption of the bubble. This produced a partial obstruction of the affected gas exchange units which manifests as regions of high $\dot{V}_A/\dot{Q}$ rather than pure dead space.

Decompression sickness
Gas exchange
Inert gas elimination
Pulmonary embolus
Ventilation/perfusion ratio

Infused venous bubble emboli produce alterations in pulmonary gas exchange that are of both practical and theoretical interest. Intravascular gas bubbles have been observed during accepted diving decompression procedures by Spencer and Clark (1972), Evans *et al.* (1972) and Neuman *et al.* (1976). These bubbles lodge in

Accepted for publication 8 September 1978

* This study was supported in part by U.S. Public Health Service grants HL 12174, HL 05372, HL 19457 and Research Career Development Award HL 00182.

the lung, but the effects on gas exchange in the lung have not been quantitated in detail. The bubble embolism model has not been utilized in the study of the more general problem of the physiological manifestations of embolism. Studies with venous thromboembolism have shown an increased physiological dead space both at rest (Stein *et al.*, 1961; Levy and Simmons, 1974) and during exercise (Nadel *et al.*, 1968), increased right-to-left shunt (Niden and Aviado, 1956), decreased diffusing capacity (Nadel *et al.*, 1968; Levy *et al.*, 1965), and changes in compliance and airways resistance (Levy *et al.*, 1965; Khan *et al.*, 1972; Josephson *et al.*, 1973). A recent study by Dantzker *et al.* (1978) described $\dot{V}A/\dot{Q}$ maldistribution produced by venous thromboemboli. Continuous bubble infusion is unique in that bubbles are continuously lodging and resolving due to gas absorption, producing a standard fraction of occluded vessels that can be readily reversed within minutes of stopping the infusion. The bubble infusion model provides a reversible model for the study of the physiology of acute vascular obstruction, and a reproducible model for the creation of alveolar dead space.

Methods

The studies were performed on ten mongrel dogs (15–25 kg), under barbiturate anesthesia (20–30 mg/kg sodium pentothal initial dose with supplemental doses of pentobarbital sufficient to prevent spontaneous respiration). The animals were ventilated with a Harvard pump ventilator at a tidal volume of 15 ml/kg. The respiratory rate was chosen to maintain an initial arterial P_{CO_2} of between 37 and 40 torr, and this rate and tidal volume were then held constant throughout the experiment. Femoral arterial and venous catheters were inserted for blood sampling, and a 7-Fr thermodilution Swan-Ganz catheter was introduced via the jugular vein and floated just distal to the pulmonic valve to permit sampling of mixed venous blood samples and to determine cardiac output. The exhaled gas was mixed in a heated 9-liter capacity 3.8 cm I.D. copper tube coil with a sampling port at the distal end. O_2 and CO_2 partial pressures at the mouth were monitored continuously with a mass spectrometer, and mixed expired partial pressures from the mixing coil were checked at 5–10-min intervals. The heart rate, pulmonary artery pressure, systemic artery pressure and exhaled gas concentrations at the mouth were recorded continuously on an eight channel recorder. P_{O_2}, P_{CO_2} and pH in arterial and mixed venous blood samples were analyzed on Radiometer blood–gas electrodes.

Nitrogen, helium or sulfur hexafluoride bubbles were infused into the femoral vein at a rate of 0.2 ml/min/kg for a period of 30 minutes using a constant flow syringe infusion pump. This embolic load was sufficient to double pulmonary artery pressure after five minutes of bubble infusion. Repeat bubble experiments with different gases were performed 90 minutes after a previous infusion provided the end-tidal P_{CO_2} and PA pressure had returned to normal 30 minutes after stopping the first infusion. The bubbles were formed by forcing gas through a PE 25

polyethylene catheter, resulting in 1.7 mm diameter bubbles produced at an approximate rate of 2000 bubbles per minute for a 25-kg dog. Bubble size was estimated *in vitro* by bubbling in plasma using a stroboscopic light to facilitate bubble size measurement with a ruler.

A dilute solution of six inert gases (sulphur hexafluoride, ethane, cyclopropane, halothane, diethyl ether, and acetone) were infused via a separate venous catheter by the method of Wagner *et al.* (1974b). The inert gas mixture was administered with infusion pump for at least 30 minutes prior to experimental run. Cardiac output was measured by the thermodilution method and minute ventilation was calculated from a 3-min collection of expired gas which was measured with a Tissot spirometer.

The concentrations of inert gases in the gas samples were measured on a gas chromatograph (Beckman GC72-5) equipped with flame ionization and electron capture (Analog Technology Corp.) detectors. The gas extraction method of Wagner *et al.* (1974a) was used to determine the concentration of the inert gases in the arterial and venous blood samples. Exhaled gas samples were heated to greater than 40 C during storage before analysis (a period of less than one hour) to avoid condensation and loss of highly soluble gases.

Raw inert gas retentions and excretions were used to calculate shunt and inert gas dead space as previously described (Hlastala and Robertson, 1978). Shunt is equal to the extrapolated limit of retention for a gas of infinitesimally low solubility. Inert gas dead space is equal to the extrapolated limit of excretion for a gas of infinitely high solubility. The arterial and alveolar P_{O_2} and P_{CO_2}, calculated from the derived VA/Q distribution (Evans and Wagner, 1977), were used to calculate an inert gas physiological dead space (Bohr equation) and a venous admixture (Berggren equation). CO_2 physiological dead space was also calculated using the Enghoff modification of the Bohr equation from measured arterial and mixed expired P_{CO_2}.

Lung specimens taken for histological examination were prepared using conventional light microscopic techniques. The lungs were inflated to 20 cm H_2O pressure and the left lower lobe artery and vein were ligated. The lobar bronchus was incised, and following collapse, the lobe was inflated with fixative. The lungs were fixed at 20 cm H_2O pressure with 10 per cent buffered formalin at 4 for 2 hours. Specimens were obtained from both dependent and upper regions of the lung. The specimens were immersed in formalin overnight, imbedded in paraffin, sectioned, and stained with hematoxylin and eosin. Luminal and periluminal measurements were made on both arterioles and venules to estimate the lumen to perivascular space ratio.

Extravascular lung water was measured using wet weight to dry weight ratios by a modification of the technique of Pearce *et al.* (1965). This method uses the hemoglobin concentration of the lung homogenate to correct for the presence of blood. A corrected wet-dry ratio was calculated for lungs from experimental animals immediately after the final bubble infusion period and from control animals anesthetized for four hours without bubble infusion.

Results

Within 0.7 minute of the initiation of 0.2 ml/kg nitrogen bubble infusion, alterations in mixed expired P_{CO_2} and pulmonary artery pressure were observed (fig. 1). Pulmonary artery pressure (PAP) increases to a peak at 8 minutes, and gradually declines. After the bubbles are stopped, pulmonary artery pressure and mixed expired P_{CO_2} return to normal with a half-time dependent upon the gas in the bubbles (see table 1).

Arterial P_{O_2} and P_{CO_2} are plotted as a function of time in fig. 2 for three different groups of experiments where either helium, nitrogen, or SF_6 bubbles were infused at a rate of 0.2 ml/kg/min for 30 minutes. The magnitude of the change produced was dependent upon the bubble gas. The half-times for both onset and resolution

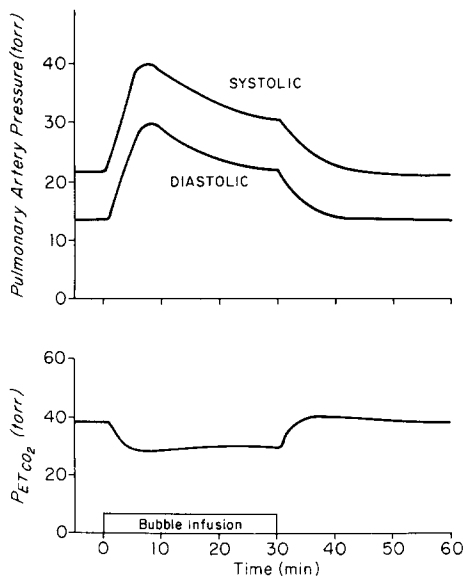

Fig. 1. Pulmonary artery pressure (systolic and diastolic) and endtidal P_{CO_2} plotted against time. Nitrogen bubble infusion at a rate of 0.2 ml/kg/min for the first 30 minutes. Data are from a single infusion in one dog.

TABLE 1
Half-times (in minutes) for change in arterial blood gases (see fig. 2)

	Onset $t_{1/2}$		Resolution $t_{1/2}$	
	P_{O_2}	P_{CO_2}	P_{O_2}	P_{CO_2}
He	4.5	8.0	7.5	15.0
N_2	4.5	8.5	11.0	16.0
SF_6	5.5	8.5	25.5	30.0

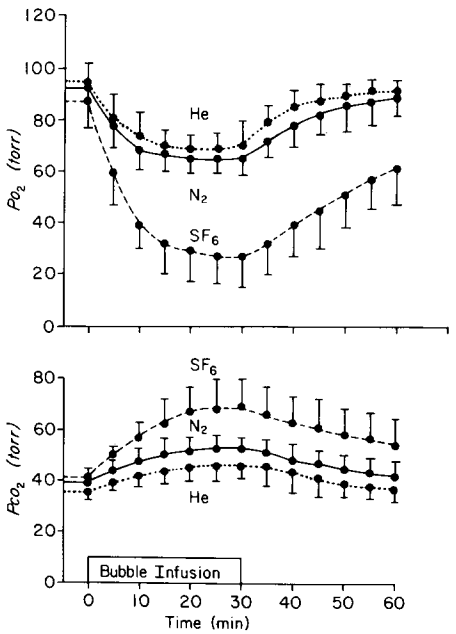

Fig. 2. Blood gas abnormalities plotted against time. Three separate groups are shown for helium, nitrogen or sulfur hexafluoride infusion. Vertical bars representing one standard deviation are shown only on one side.

with helium and nitrogen bubbles (table 1) are similar; whereas the time of resolution of sulfur hexafluoride bubbles is much greater. The gas exchange abnormalities for both the helium and nitrogen experiments are shown in table 2. The alveolar–arterial oxygen difference more than doubled during bubble infusion. A marked increase in physiological dead space was also documented.

A representation of the ventilation to perfusion distribution changes (fig. 3) was obtained using the smoothing inversion algorithm of Wagner *et al.* (1975). In fig. 3A before the bubble infusion is started, the $\dot{V}_A/\dot{Q}$ distribution is normal (Hlastala *et al.*, 1975; Wagner *et al.*, 1975) with a mean $\dot{V}_A/\dot{Q}$ of 0.9. There is no ventilation to regions with $\dot{V}_A/\dot{Q}$ ratios greater than 5.0. Note that there is no shunt and the inert gas V_D/V_T, representing instrument and anatomic dead space, (Hlastala and Robertson, 1978) is 0.4. After 15 minutes of embolization (fig. 3B), there is preservation of ventilation and perfusion at the normal ratios. The striking observation is that there has been a very large fraction of ventilation redistributed to high $\dot{V}_A/\dot{Q}$ regions with no change in the inert gas dead space. The distribution obtained at 30 minutes after embolization (fig. 3C) is nearly identical to that after 15 minutes. Fifteen minutes after cessation of bubble infusion (fig. 3D), the ventilation peak in the high $\dot{V}_A/\dot{Q}$ regions is smaller and its overall $\dot{V}_A/\dot{Q}$ ratio is slightly lower than during infusion. Again, pure dead space has remained constant. Finally, 30 minutes after cessation of bubble infusion (fig. 3E), the lung has returned nearly to normal

TABLE 1
Time from control (min)

	0 (Control)	15 (Infusion)	30 (Infusion)	45 (Resolution)	60 (Resolution)
Pulmonary artery Mean pressure (torr)	17.5 ± 6.6	**30.1 ± 12.7	*25.4 ± 14.3	16.4 ± 7.9	14.7 ± 6.9
Cardiac output (L/min)	5.8 ± 2.6	5.3 ± 2.0	4.5 ± 1.9	4.5 ± 2.3	4.1 ± 1.8
$(A-a)D_{O_2}$ (torr)	13.6 ± 12.0	***32.8 ± 11.2	***31.7 ± 9.3	16.4 ± 12.0	16.3 ± 12.2
Venous admixture ($\dot{Q}va/\dot{Q}t$) (%)	15.3 ± 6.5	**33.8 ± 14.8	***31.6 ± 11.2	16.0 ± 7.1	12.2 ± 6.6
Shunt ($\dot{Q}s/\dot{Q}t$) (%)	2.5 ± 3.9	1.3 ± 2.2	2.4 ± 2.8	1.7 ± 2.4	1.6 ± 2.7
Inert Gas V_D/V_T (%)	41.8 ± 5.9	39.6 ± 5.0	39.4 ± 3.8	42.3 ± 6.4	41.3 ± 8.2
Physiologic V_D/V_T (From inert gases) (%)	55.5 ± 7.3	***67.1 ± 6.7	***65.4 ± 7.2	59.5 ± 8.8	54.4 ± 10.9
Physiologic V_D/V_T (From CO_2) (%)	48.4 ± 9.5	***62.2 ± 9.0	***61.5 ± 8.2	50.3 ± 12.2	47.6 ± 12.1

Combined variables for He and N_2 infusion experiments.
Significance levels (compared to control).
* $P < 0.01$.
** $P < 0.005$.
*** $P < 0.001$.
All others are not significant at $P > 0.05$ level.

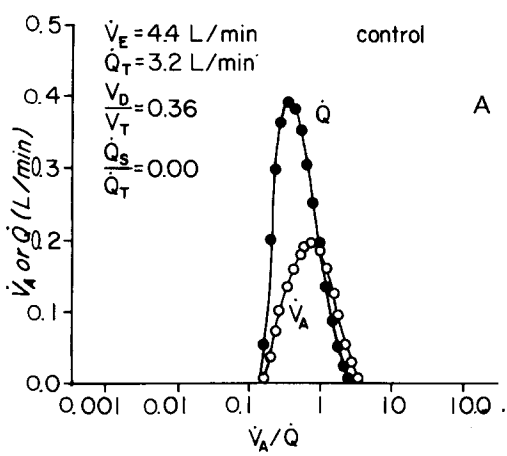

Fig. 3. $\dot{V}_A/\dot{Q}$ distributions obtained from single run of nitrogen bubble infusion in one dog. (3A) Control before bubble infusion; (3B) After fifteen minutes of bubble infusion; (3C) After thirty minutes of bubble infusion; (3D) Fifteen minutes after stopping infusion; (3E) Thirty minutes after stopping infusion.

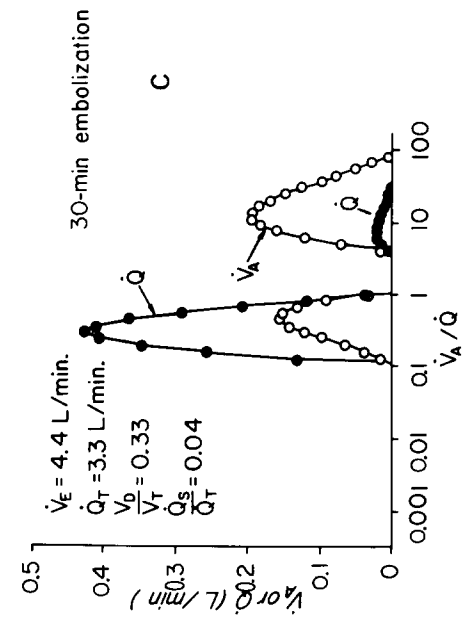
30-min embolization
C
$\dot{V}_E$ = 4.4 L/min.
$\dot{Q}_T$ =3.3 L/min.
$\frac{V_D}{V_T}$ = 0.33
$\frac{\dot{Q}_S}{\dot{Q}_T}$ = 0.04
$\dot{V}_A$ or $\dot{Q}$ (L/min)
$\dot{V}_A/\dot{Q}$
0.5
0.4
0.3
0.2
0.1
0
0.001 0.01 0.1 1 10 100

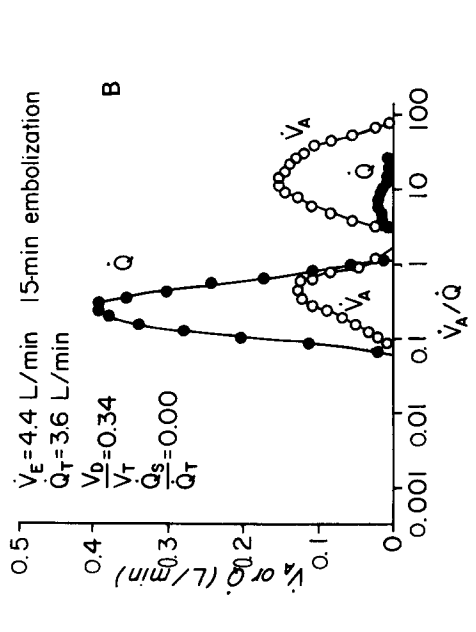
15-min embolization
B
$\dot{V}_E$=4.4 L/min
$\dot{Q}_T$=3.6 L/min
$\frac{V_D}{V_T}$=0.34
$\frac{\dot{Q}_S}{\dot{Q}_T}$=0.00
$\dot{V}_A$ or $\dot{Q}$ (L/min)
$\dot{V}_A/\dot{Q}$
0.5
0.4
0.3
0.2
0.1
0
0.001 0.01 0.1 1 10 100

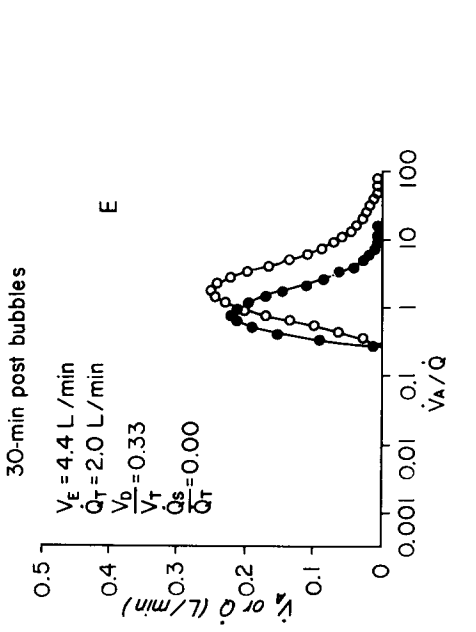
30-min post bubbles
E
$\dot{V}_E$ = 4.4 L/min
$\dot{Q}_T$ = 2.0 L/min
$\frac{V_D}{V_T}$ = 0.33
$\frac{\dot{Q}_S}{\dot{Q}_T}$ = 0.00
$\dot{V}_A$ or $\dot{Q}$ (L/min)
$\dot{V}_A/\dot{Q}$
0.5
0.4
0.3
0.2
0.1
0
0.001 0.01 0.1 1 10 100

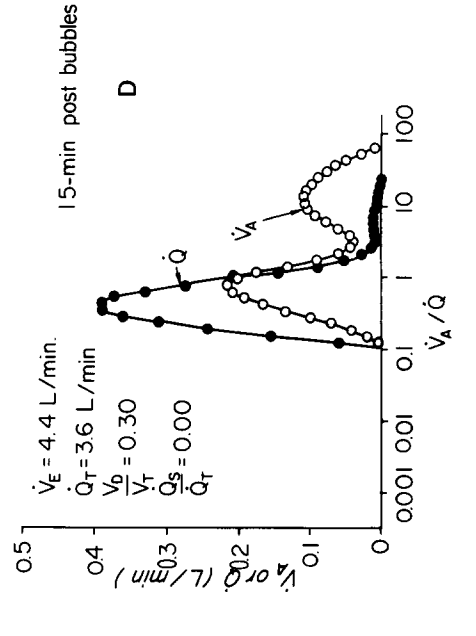
15-min post bubbles
D
$\dot{V}_E$ = 4.4 L/min.
$\dot{Q}_T$ = 3.6 L/min
$\frac{V_D}{V_T}$ = 0.30
$\frac{\dot{Q}_S}{\dot{Q}_T}$ = 0.00
$\dot{V}_A$ or $\dot{Q}$ (L/min)
$\dot{V}_A/\dot{Q}$
0.5
0.4
0.3
0.2
0.1
0
0.001 0.01 0.1 1 10 100

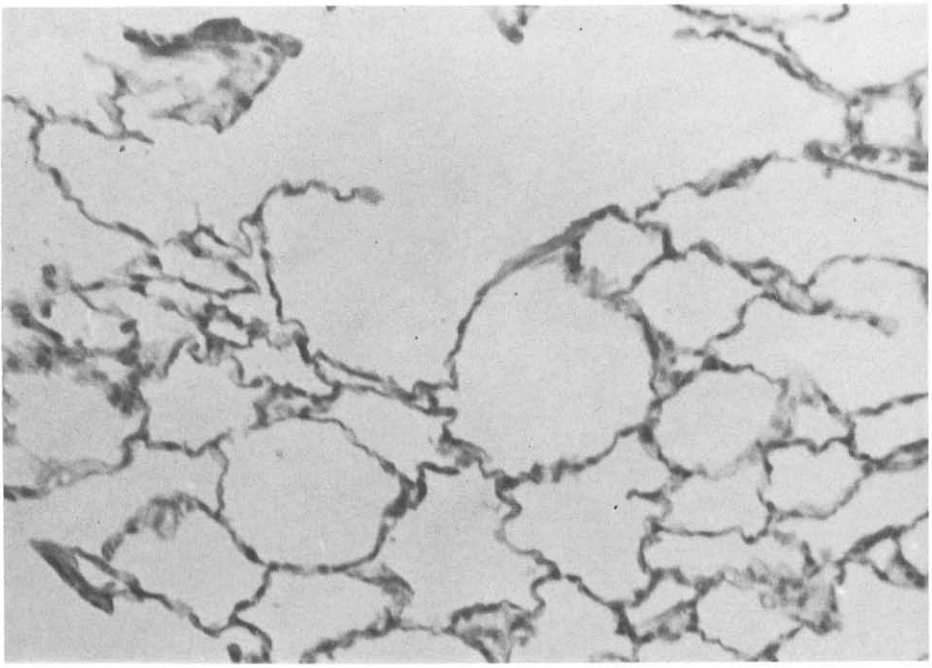

A

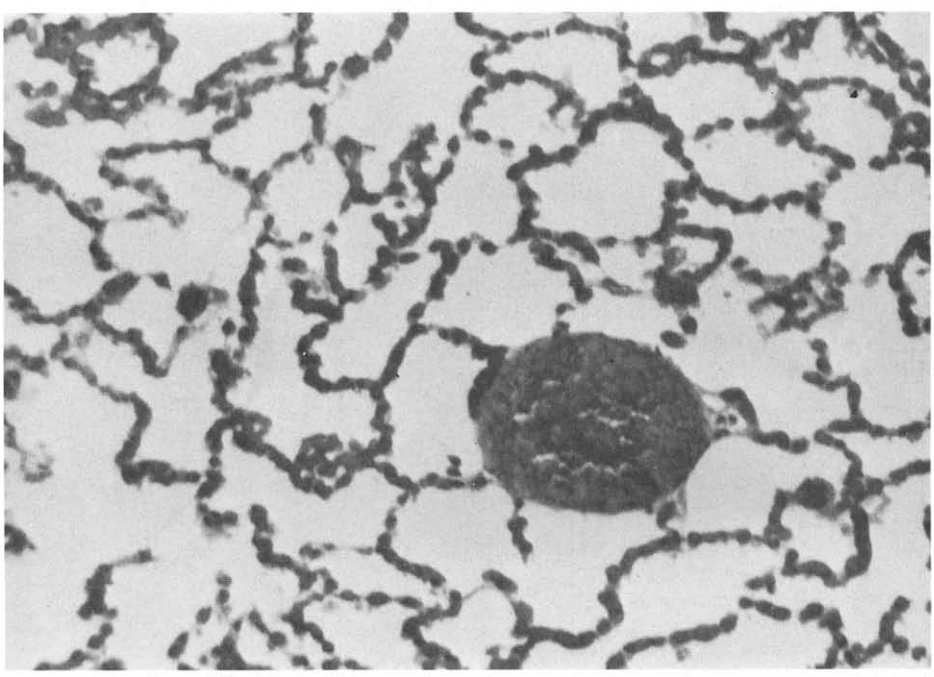

B

Fig. 4. Histological sections of control lung (4A) and of lung after two separate 30-min infusions of nitrogen bubbles (4B). Both are taken from a similar area in the upper portion of the lung. After embolization, vascular engorgement is seen. But there is little evidence of interstitial or alveolar edema. Original magnification × 1240.

in terms of $\dot{V}_A/\dot{Q}$ ratio distribution, except for the slight skewness toward high $\dot{V}_A/\dot{Q}$.

The wet weight/dry weight ratios of lungs sampled during embolization were measured and found to be significantly greater than control lungs (4.81 ± 0.53 *versus* 3.53 ± 0.72, $P < 0.01$). Histological examination of the bubble embolized lungs showed an increase in vascular engorgement (fig. 4B), as compared to control (Fig. 4A), but no apparent increase in the area of the perivascular space. Hence, there was no consistent histological evidence of interstitial edema in spite of the increased wet/dry weight ratio. We found no alveolar edema except in one instance where a high SF_6 embolization rate (0.6 ml/kg/min) resulted in the death of the animal.

Discussion

Gas bubble embolization differs from thromboemboli and glass bead emboli in that the bubbles are in a constant state of change by virtue of growth or resolution. As the nitrogen bubbles enter the blood stream, they begin to equilibrate with blood partial pressures of oxygen, carbon dioxide and nitrogen. This exchange process is complex not only because it is a three gas system with each gas moving independently, but also because of the complex convective features of the gas–blood boundary layer established at the bubble surface (Hlastala and Farhi, 1973). The bubbles presumably lodge initially in large pulmonary arterioles. Since the partial pressure of inert gas within the bubble is greater than that in the blood, tissue, or alveolar space, the bubble will begin to resolve and slip further down the vasculature. Furthermore, as both systemic (Buckles, 1968) and pulmonary (Knisely, 1969) bubble emboli have been demonstrated to elongate within the vasculature, bubbles will probably not remain spherical but will deform as they are pushed further down into smaller vessels affecting smaller lung regions. In this set of experiments, a steady state is reached after approximately 15 minutes, in that the alteration in gas exchange remains constant. Presumably, a steady state of obstruction is then produced, where the rate of delivery of bubbles embolizing regions of the lung is balanced by the resolution of earlier embolized regions.

When the bubbles resolve to a point where they are sufficiently small, they may have the opportunity to slip into the pulmonary venous circulation. However it remains to be established whether small bubbles can slip through or whether they remain in the pulmonary capillary until totally resolved. In the situation where the bubbles result from decompression, bubble passage into the arterial system could be detrimental. The arterial bubbles would come in contact with supersaturated blood and could grow again, resulting in arterial embolization.

ALTERED GAS CLEARANCE

The results of this study partially answer the practical question of whether nitrogen bubble emboli produced during decompression sickness help or hinder the elimination of nitrogen. In fig. 5 the retention and excretion ratios are plotted against solubility for each of the experimental gases in a normal dog lung both before and after embolization. In the pre-embolization period, the arterial or retention value exceeds the mixed expired or excretion value by virtue of normal $\dot{V}_A/\dot{Q}$ heterogeneity and inert gas dead space (for details, see Hlastala and Robertson, 1978). After embolization, the retention of each gas is increased and the excretion is reduced. Using the retention curve, the effect of embolism on clearance of nitrogen (solubility in blood = 0.0122 ml/ml/atm) during 100% oxygen breathing can be quantitated. The normal retention of nitrogen in blood going through the lung is approximately 4%, so that 96% of the nitrogen is cleared in passage through the normal lung. With embolization, the retention of nitrogen is nearly doubled, dropping the clearance to roughly 93%. Hence bubble embolization during decompression is detrimental to the elimination of supersaturated inert gas.

Of the inert gases used in diving, all are of relatively low solubility and, hence, the clearance is more dependent upon perfusion rather than ventilation (Farhi, 1967) so the effect of shifting of ventilation on clearance is relatively small. However, the elimination process is highly dependent upon perfusion and thus a sufficient embolic load to decrease the cardiac output could compromise the clearance of a low solubility gas. In most of the animals we found that embolization caused a slight decrease in cardiac output which was not significant (table 2).

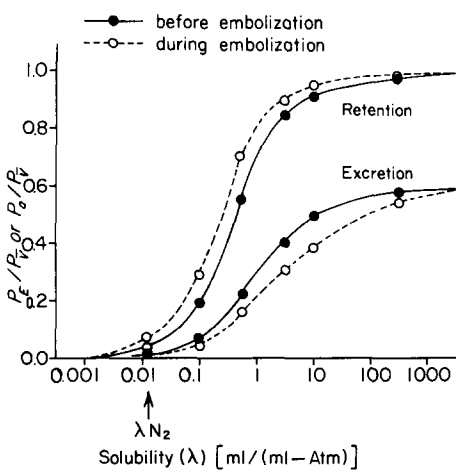

Fig. 5. Retention and excretion curves for the lungs depicted in fig. 3. Solid lines are from control lung before embolization. Dashed lines are from lung after fifteen minutes of bubble infusion. Solubility of nitrogen is indicated by vertical arrow (see text).

DEAD SPACE

The primary gas exchange abnormality demonstrated in this study was the creation of regions with high $\dot{V}A/\dot{Q}$ ratios without a change in inert gas dead space (fig. 3). It seems surprising that embolization did not increase the inert gas dead space, but two factors could explain this finding. First, large blood vessels would only be transiently blocked by the rapidly resolving bubbles. The smaller bubbles would slide into smaller vessels lodging in areas which could receive perfusion from other microvessels. Second, small peripheral parallel alveolar dead space units produced by bubble emboli would have to inspire through series anatomic dead space which contains gas expired from parallel perfused regions. Ross and Farhi (1960) have shown that such regions tend to average the gas exchange properties of disparate peripheral units. Hence, it is probable that parallel dead space units may, in the presence of series dead space, appear as high $\dot{V}A/\dot{Q}$ units (an average of normal units and parallel dead space). The latter hypothesis would be consistant with our finding of a slightly reduced inert gas dead space during bubble infusion (table 2) if initial parallel dead space is being made to appear like high $\dot{V}A/\dot{Q}$ units. The decrease in inert gas dead space after embolization was only significant at the $P < 0.1$ level however. An alternate explanation for the drop in inert gas dead space is that reflex bronchial constriction is causing a slight decrease in anatomic dead space. Bronchial constriction and increased airway resistance has previously been shown with embolization (Khan *et al.*, 1972).

Although the changes in the inert gas dead space were small, the inert gas physiological dead space (Bohr VD/VT) as calculated from the Wagner computer program increased from 55.5% to 67.1% (table 2) with embolization. The CO_2 VD/VT (Bohr VD/VT) calculated from the directly measured Pa_{CO_2} and PE_{CO_2} increased

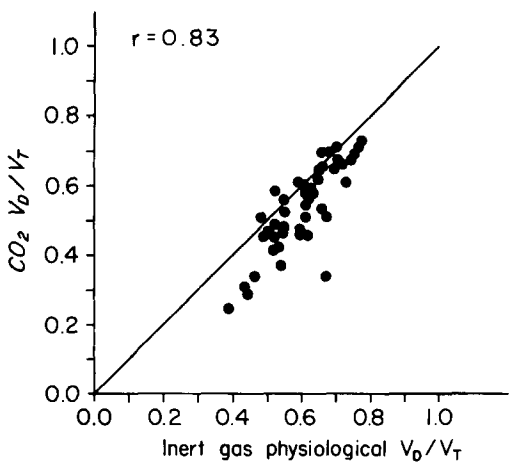

Fig. 6. Physiological dead space/tidal volume ratio determined with CO_2 plotted against CO_2 physiological dead space ratio determined from inert gases. The line of identity is shown. Inert gas physiological VD/VT significantly ($P < 0.001$) exceeds CO_2 physiological VD/VT.

from 48.4% to 62.2%. The difference between these two measurements shown in fig. 6 is significant ($P < 0.001$) but the calculated change with embolization is roughly the same (11.6% for predicted V_D/V_T change compared to 13.8% for measured V_D/V_T change). The differences between the predicted and measured physiological dead space measurements is consistent with our previous findings which used another approach to calculation of the predicted $P_{E_{CO_2}}$ from inert gas data (Robertson and Hlastala, 1977). Both CO_2 and the inert gases are loaded into the venous blood, and there is no reason to suppose that the V_D/V_T for CO_2 or an inert gas of identical solubility should differ if passive diffusion were the only determinant of equilibration between alveolar gas and pulmonary capillary blood. This provides support for the finding that there is active elimination of CO_2 from the lung during normal respiration.

HYPOXEMIA

Of the causes of hypoxemia, ventilation perfusion maldistribution plays the major role. Intrapulmonary shunt was small (averaging 2.5%) and did not change significantly either during embolization or after embolization. In addition, it is unlikely that diffusion equilibration limitation existed, as any significant oxygen diffusion limitation would have resulted in a discrepancy between predicted (from inert gas $\dot{V}_A/\dot{Q}$ distributions) and measured arterial P_{O_2}. Figure 7 shows the predicted P_{O_2} plotted against measured arterial P_{O_2}. There was no significant difference between the two and the correlation coefficient was large. Figure 3 shows a marked alteration in $\dot{V}_A/\dot{Q}$ distribution with large amounts of ventilation going to very high $\dot{V}_A/\dot{Q}$ regions. With embolization and constant cardiac output, there was a relative increase in blood flow through the normal regions resulting in a lower mean $\dot{V}_A/\dot{Q}$ of these

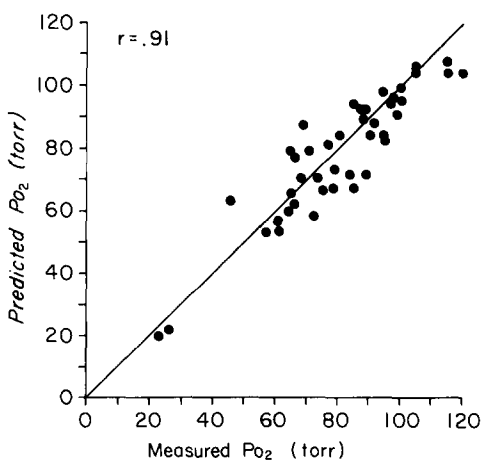

Fig. 7. Predicted arterial P_{O_2} (from inert gases) plotted against measured arterial P_{O_2}. Solid line is line of identity.

regions, causing the hypoxemia observed in fig. 2. This is consistent with the observations of Dantzker *et al.* (1978) using autologous thromboemboli and the conclusions of Verstappen *et al.* (1977) using bubble infusion.

TIME COURSE

The rate of change of blood gases at the onset of embolization is independent of the type of gas in the bubbles (table 1), but the half-times of change occurring after stopping the bubble infusion are dependent on the physical properties of the gases within the ubbles. The dynamics are complex and depend heavily on the type of tissue surrounding a lodged bubble (Hlastala and Van Liew, 1975) or the blood flow around an intravascular bubble (Hlastala and Farhi, 1973). The half-time of resolution for P_{O_2} and P_{CO_2} is similar for either helium or nitrogen bubbles. The rate of change for P_{O_2} is faster than for P_{CO_2}. The time of resolution of SF_6 bubbles is considerably greater than He or N_2 bubbles due to the high molecular weight and very low diffusivity of SF_6. Once infused, these bubbles grow as N_2 diffuses in faster than SF_6 diffuses out of the bubbles during the initial transient state. Then, after N_2 influx, the resolution due to N_2 and SF_6 efflux is much slower than pure N_2 bubbles because of the low diffusivity of SF_6 (Van Liew and Passke, 1967).

The pulmonary artery pressure peaks within eight minutes of initiation of constant bubble infusion (fig. 1) and then drops to a mean of 30.1 torr after 15 minutes (table 2) and then down to 25.4 torr after 30 minutes of bubble infusion. This is in contrast to Spencer and Oyama (1971) who found a continual increase in pulmonary artery pressure after 30 minutes of nitrogen bubble infusion at a rate of 0.15 ml/kg/min in sheep. The increase in pulmonary artery pressure with embolization is not solely due to mechanical obstruction of blood vessels (Hyland *et al.*, 1963; Josephson *et al.*, 1973). Platelet adhesion to the bubble surface (Philp *et al.*, 1972) may result in the release of vasoactive substances when lodged in the lung which may contribute to vasoconstriction with both bubble emboli (Khan *et al.*, 1972) and thromboemboli (Levy *et al.*, 1969; Malik and van der Zee, 1977). Levy *et al.* (1969) showed a drop in the humoral vasoactive contribution to the increase in pulmonary artery pressure within 30 minutes in dogs. This is consistent with the decrease in pulmonary artery pressure seen in our experiments after 30 minutes in spite of a continuous bubble infusion.

PULMONARY EDEMA

A deleterious effect of embolization is the production of pulmonary edema. It has been proposed that this may be due to the release of substances which increase pulmonary vascular permeability (Fishman and Pietra, 1974; Saldeen, 1976; Stein and Levy, 1974). Edema production may also be enhanced by the nonuniform

increases in pulmonary vascular resistance such that some unobstructed microvessels are exposed to increased hydrostatic pressure (Okuda *et al.*, 1976). In the present study, we found a significant increase in wet weight/dry weight ratio from 3.53 $\pm$ 0.72 in control lungs to 4.81 $\pm$ 0.53 in embolized lungs. This maneuver was sufficient to increase lung water but was not adequate to cause perivascular cuffing. It may be that there was insufficient time during the two one-half hour bubble exposures for enough fluid to move from the interstitium to the perivascular space or alternatively, lymphatic drainage may have been adequate at this early stage of edema.

ANALYSIS OF INERT GAS ELIMINATION DATA

The data presented was analyzed using Wagner's 50 compartment lung model (Evans and Wagner, 1977) and by a simpler four compartment lung model: pure shunt (Q_1), pure dead space (V_{A_4}) and two compartments with finite $\dot{V}_A/\dot{Q}$ between 0.001 and 100. The intermediate compartments were allowed to vary and seek a position on the $\dot{V}_A/\dot{Q}$ scale to minimize the error between model calculated and experimentally measured retentions and excretions in a manner similar to Wagner *et al.* (1974b) with their fixed fifty compartment model. Since there are six unknows (Q_1, Q_2, Q_3, V_{A_2}, V_{A_3}, V_{A_4}; $Q_4 = 0$. and $V_{A_1} = 0$) and six data points (the combined retention and excretion for each of six gases), only one solution exists. Using this approach, we obtained the solution shown in table 3 from the same data used in fig. 3C, which are analogous to the solution obtained using Wagner's algorithm. The resulting tabular representation for the four units is similar to the continuous distribution but with each mode condensed to a vertical bar at one single $\dot{V}_A/\dot{Q}$ which lies in the middle of the mode.

A third approach is to utilize the raw experimental data for retention and excretion of each inert gas. A detailed analysis of this approach is presented elsewhere (Hlastala and Robertson, 1978). It is possible to calculate physiological dead space, venous admixture and alveolar–arterial difference for each gas. The existence of low $\dot{V}_A/\dot{Q}$ units results in a marked increase in retention of low solubility gases. The existence of high $\dot{V}_A/\dot{Q}$ units results in a marked decrease in

TABLE 3
Four compartment fit to same data as in fig. 3C

Compartment	$\dot{V}_A/\dot{Q}$	$\dot{V}_A$	$\dot{Q}$
1	0	0	0.135
2	0.307	0.918	2.989
3	11.371	1.998	0.176
4	∞	1.524	0
	Total	4.440 L/min	3.300 L/min

excretion of high solubility gases. As $\dot{V}_A/\dot{Q}$ heterogeneity increases, the area under the alveolar–arterial difference *vs.* solubility curve increases. The position of the alveolar-arterial difference *vs.* solubility curve relative to the mean $\dot{V}_A/\dot{Q}$ of the lung is determined by the skewness of the $\dot{V}_A/\dot{Q}$ distribution.

Each one of these approaches to the interpretation of inert gas data has its inherent advantages and disadvantages and we, therefore, find ourselves using all three. The Wagner approach for displaying $\dot{V}_A/\dot{Q}$ distributions is used as the primary form of presentation (fig. 3) in this study because the changes are more apparent. However, one must be cautious not to overinterpret the precise shapes of these distributions.

This study demonstrates significant alterations in pulmonary gas exchange with the filtering of venous gas bubbles. A marked shift of ventilation to higher $\dot{V}_A/\dot{Q}$ regions and a shift of perfusion to low $\dot{V}_A/\dot{Q}$ regions lead to serious deficits in O_2 and CO_2 exchange capabilities of the lung. Although this produces only a minor reduction in the capacity of the lungs to eliminate low solubility inert gases, the potential also exists for serious long term effects due to pulmonary edema following more prolonged exposure to venous gas emboli. The bubble embolism preparation provides a readily reversible model for the study of the acute effects of pulmonary vascular occlusion. It is also of physiologic interest in that it provides a simple model for the creation or removal of alveolar dead space.

Acknowledgements

The capable technical assistance of Rosa Linda Franada, Wayne Kirk, Pam McKenna, John Mendenhall and Dave Simmons is gratefully acknowledged.

References

Buckles, R. G. (1968). The physics of bubble formation and growth. *Aerosp. Med.* 38: 1062–1069.

Dantzker, D. R., P. D. Wagner, V. W. Tornabene, N. P. Alazraki and J. B. West (1978). Gas exchange after pulmonary thromboembolization in dogs. *Circ. Res.* 42: 92–102.

Evans, A., E. E. P. Barnard and D. N. Walder (1972). Detection of gas bubbles in man at decompression. *Aerosp. Med.* 43: 1095–1096.

Evans, J. W. and P. D. Wagner (1977). Limits on V_A/Q distributions from analysis of experimental inert gas elimination. *J. Appl. Physiol.* 42: 889–898.

Farhi, L. E. (1967). Elimination of inert gas by the lung. *Respir. Physiol.* 3: 1–11.

Fishman, A. P. and G. G. Pietra (1974). Handling of bioactive materials by the lung. *New Engl. J. Med.* 291: 884–990.

Hlastala, M. P. and L. E. Farhi (1973). Absorption of gas bubbles in flowing blood. *J. Appl. Physiol.* 35: 311–316.

Hlastala, M. P., P. S. Colley and F. W. Cheney (1975). Pulmonary shunt: a comparison between oxygen and inert gas infusion methods. *J. Appl. Physiol.* 39: 1048–1051.

Hlastala, M. P. and H. D. Van Liew (1975). Absorption of *in vivo* inert gas bubbles. *Respir. Physiol.* 24: 147–158.

Hlastala, M. P. and H. T. Robertson (1978). Inert gas elimination characteristics of the normal and abnormal lung. *J. Appl. Physiol.* 44: 258–266.

Hyland, J. W., T. E. Piemme, S. Alexander, F. W. Haynes, G. T. Smith and L. Dexter (1963). Behavior of pulmonary hypertension induced by serotonin and emboli. *Am. J. Physiol.* 205: 591–597.

Josephson, S., E. Berglund, T. C. McAslan, M. Mima and P. Herzog (1973). Lung mechanics and respiratory gas exchange during pulmonary air embolization in the dog. *Scand. J. Clin. Lab. Invest.* 32: 265–270.

Khan, M. A., I. Alkalay, S. Suetsugu and M. Stein (1972). Acute changes in lung mechanics following pulmonary emboli of various gases in dogs. *J. Appl. Physiol.* 36: 60–68.

Knisely, W. H. (1969). Normal morphology and some defined pathologic conditions of fine vessels of mammalian alveoli. In: The Microcirculation, ed. by W. K. Winters and A. N. Brest. Springfield, IL, Charles C. Thomas, pp. 159–173.

Levy, S. E., M. Stein, R. S. Totten, I. Bruderman, S. Wessler, and E. D. Robin (1965). Ventilation-perfusion abnormalities in experimental pulmonary embolism. *J. Clin. Invest.* 44: 1699–1707.

Levy, S. E., B. J. Shapiro and D. H. Simmons (1969). Pulmonary hemodynamics after autologous *in vivo* pulmonary thromboembolism. *J. Appl. Physiol.* 27: 53–60.

Levy, S. E. and D. H. Simmons (1974). Redistribution of alveolar ventilation following pulmonary thromboembolism in the dog. *J. Appl. Physiol.* 36: 60–68.

Malik, A. B. and H. van der Zee (1977). Time course of pulmonary vascular response to micro-embolization. *J. Appl. Physiol.* 43: 51–58.

Nadel, J. A., W. M. Gold and J. H. Burgess (1968). Early diagnosis of chronic pulmonary vascular obstruction. *Am. J. Med.* 44: 16–25.

Neuman, T. S., D. A. Hall and P. G. Linaweaver, Jr. (1976). Gas phase separation during decompression in man: ultrasound monitoring. *Undersea Biomed. Res.* 3: 121–130.

Niden, A. H. and D. M. Aviado, Jr. (1956). Effects of pulmonary embolism on the pulmonary circulation with special reference to arteriovenous shunts in the lung. *Circ. Res.* 4: 67–73.

Okuda, K., K. Nakahara and N. C. Staub (1976). Changes in lung fluid and protein balance in sheep after microembolism. *Physiologist* 19: 315.

Pearce, M. L., J. Yamashita and J. Beazell (1965). Measurement of pulmonary edema. *Circ. Res.* 16: 482–488.

Philp, R. B., M. J. Inwood and B. A. Warren (1972). Interactions between gas bubbles and components of the blood: Implications in decompression sickness. *Aerosp. Med.* 43: 946–953.

Robertson, H. T. and M. P. Hlastala (1977). Anomalous elevation of alveolar P_{CO_2} in normal breathing dogs. *J. Appl. Physiol.* 43: 357–364.

Ross, B. B. and L. E. Farhi (1960). Dead-space ventilation as a determinant in the ventilation–perfusion concept. *J. Appl. Physiol.* 15: 363–371.

Saldeen, T. (1976). Microembolism syndrome. *Microvasc. Res.* 11: 227–259.

Spencer, M. P. and D. Oyama (1971). Pulmonary capacity for dissipation of venous gas emboli. *Aerosp. Med.* 42: 822–827.

Spencer, M. P. and H. F. Clark (1972). Precordial monitoring of pulmonary gas embolism and decompression sickness. *Aerosp. Med.* 43: 762–767.

Stein, M., C. E. Forkner, E. D. Robin and S. Wessler (1961). Gas exchange after autologous pulmonary embolism in dogs. *J. Appl. Physiol.* 16: 488–492.

Stein, M. and S. E. Levy (1974). Reflex and humoral responses to pulmonary embolism. *Progr. Cardiovasc. Dis.* 17: 167–174.

Van Liew, R. D. and M. Passke (1967). Permeation of neon, nitrogen and sulfur hexafluoride through walls of subcutaneous gas pockets in rats. *Aerosp. Med.* 38: 829–831.

Verstappen, F. J. J., J. A. Bernards and F. Kreuzer (1977). Effects of pulmonary gas embolism on circulation and respiration in the dog. IV. Origin of arterial hypoxemia during pulmonary gas embolism. *Pflügers Arch.* 370: 71–75.

Wagner, P. D., P. F. Naumann and R. D. Laravuso (1974a). Simultaneous measurement of eight foreign gases in blood by gas chromatography. *J. Appl. Physiol.* 36: 600–605.

Wagner, P. D., H. A. Saltzman and J. B. West (1974b). Measurement of continuous distributions of ventilation-perfusion ratios: theory. *J. Appl. Physiol.* 36: 588–599.

Wagner, P. D., R. B. Laravuso, E. Goldzimmer, P. F. Naumann and J. B. West (1975). Distributions of ventilation–perfusion ratios in dogs with normal and abnormal lungs. *J. Appl. Physiol.* 38: 1099–1109.